Electronic Supplementary Material (ESI) for Energy & Environmental Science.

Efficient Charge Extraction and Slow Recombination in Organic-Inorganic Perovskites Capped with Semiconducting Single-walled Carbon Nanotubes

Rachelle Ihly, Anne-Marie Dowgiallo, Mengjin Yang, Philip Schulz, Noah Stanton, Obadiah Reid, Andrew Ferguson, Kai Zhu, Joseph J. Berry, Jeffrey L. Blackburn*

National Renewable Energy Laboratory, Golden, CO 80401
Chemical and Materials Science Center

Supporting Information

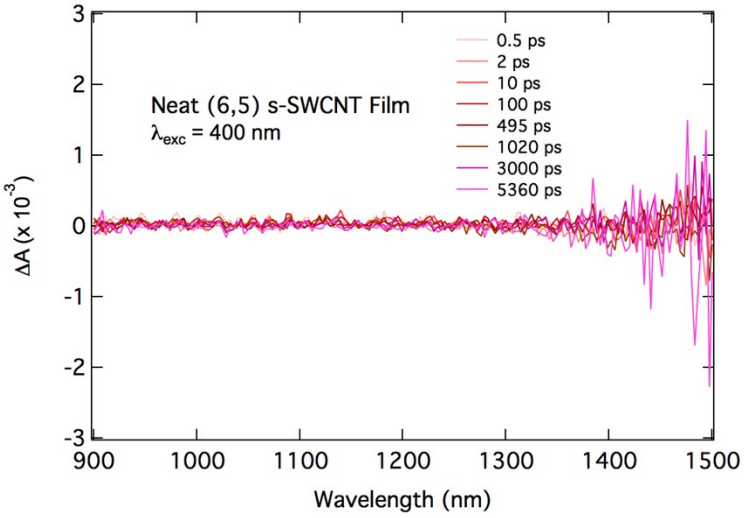

Figure S1. Control pump-probe experiment showing TA spectra for neat (6,5) s-SWCNT thin film (10 nm) pumped at 400 nm with fluence of 2 x 10^{11} photons/cm^2/pulse. This fluence corresponds to the illumination intensity seen by the SWCNT HTL following Beer-Lambert decay through the MAPI layer upon "backside" illumination for trilayer samples measured in the main manuscript. The control experiment demonstrates that no signal can be seen for the s-SWCNTs under these illumination conditions, confirming that all signal in the SWCNT layer for a trilayer (TiO_2/MAPI/SWCNT) sample results from hole transfer from the photoexcited $MAPbI_3$ layer into the SWCNT thin film.

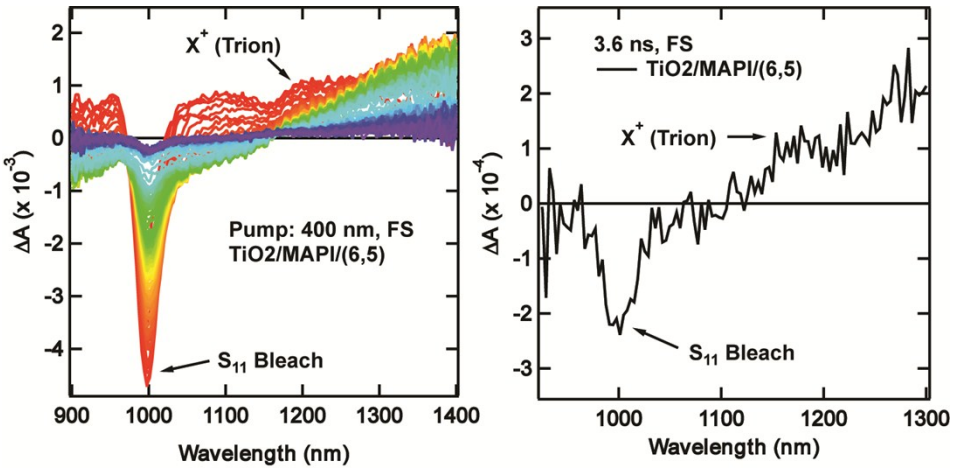

Figure S2. Representative TA spectra for a frontside illumination experiment on a TiO_2/$MAPbI_3$/(6,5) trilayer sample.

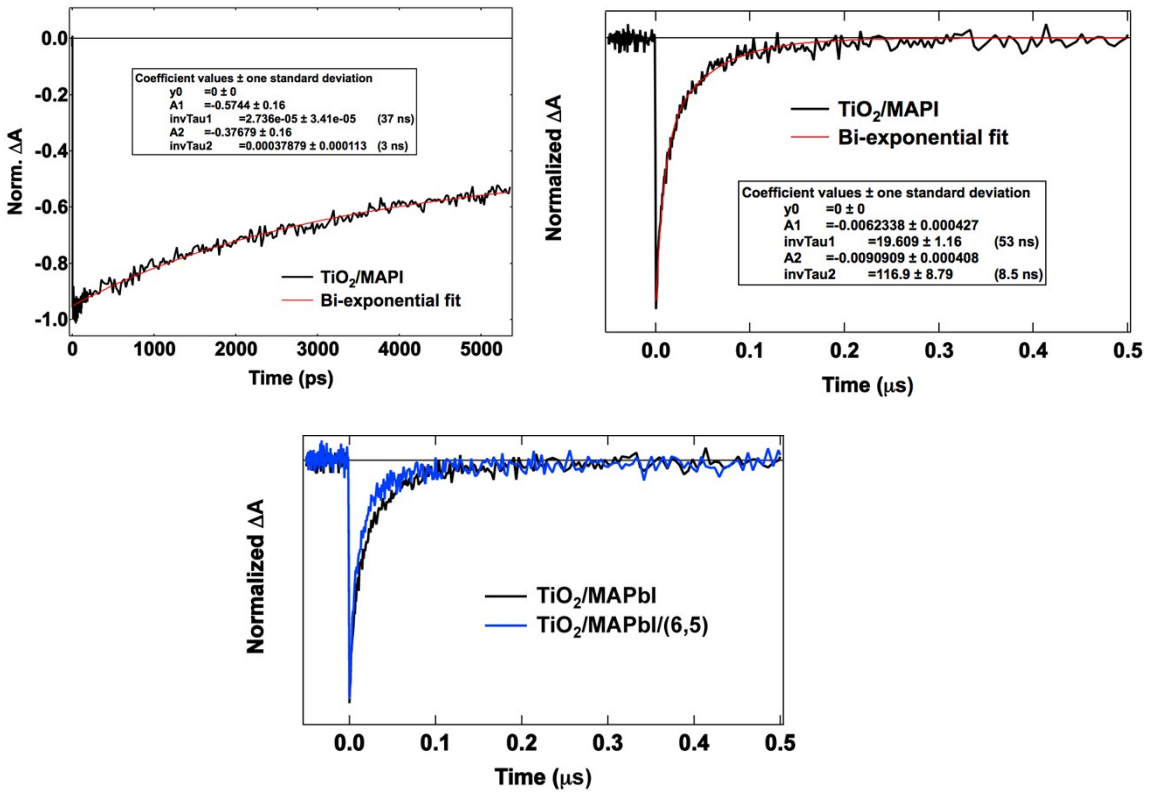

Figure S3. (a) 'Short-delay' TA dynamics (t < 5.4 ns) and (b) 'long-delay' TA dynamics (t < 500 μs) for the bilayer (TiO_2/$MAPbI_3$) sample following photoexcitation at 400 nm. The transient is fit by a biexponential decay, with time constants of τ_1 = 8 ns and τ_2 = 50 ns. (c) Comparison of normalized kinetics at 750 nm for samples pumped at 400 nm over the first 500 ns.

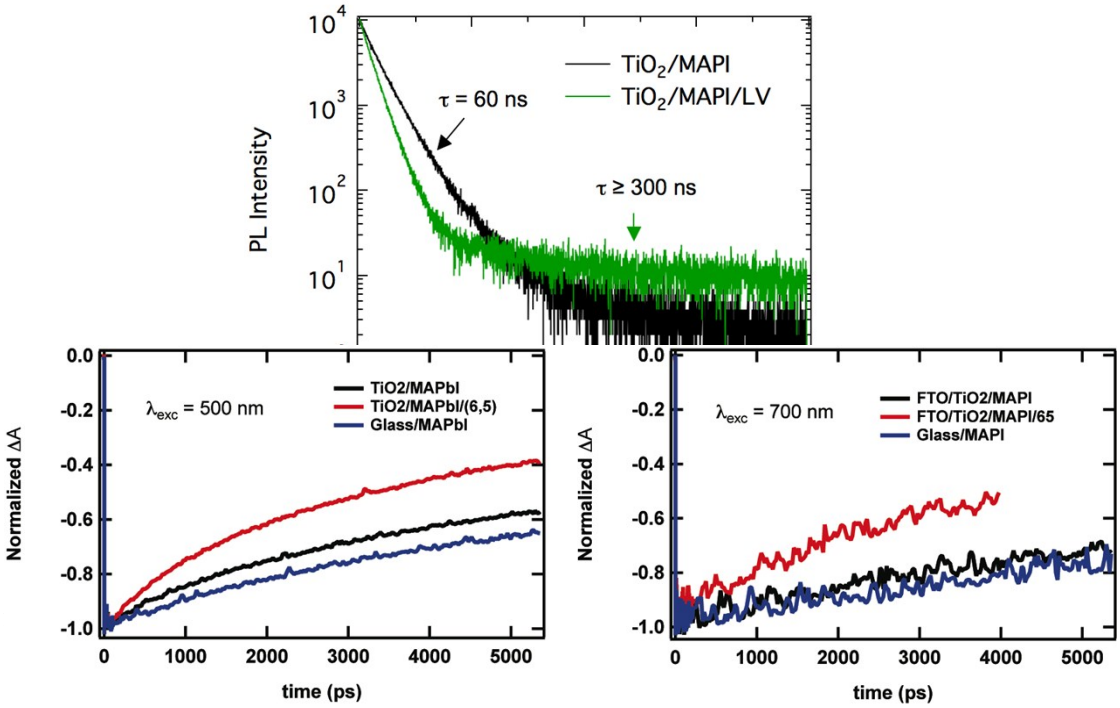

Figure S5. Comparison of Kinetics at 750 nm for samples pumped at (a) 700 nm and (b) 500 nm. In both cases, the results are similar to those reported in the main manuscript for 400 nm excitation: samples with the (6,5) SWCNT HTL exhibit faster bleach recovery than those without the (6,5) HTL.

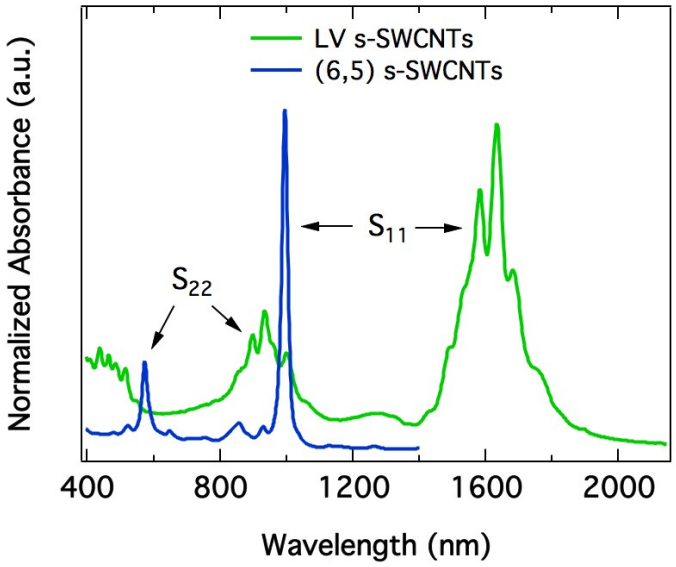

Figure S6. Optical absorption spectra for (6,5) s-SWCNTs and LV s-SWCNTs, both dispersed with PFO-BPy in toluene. The optical band gap of the (6,5) s-SWCNTs is ca. 1.25 eV, with an electrical band gap of ca. 1.52 eV. The optical band gap of the LV s-SWCNTs is ca. 0.77 eV, with an electrical band gap of ca. 0.92. The electrical band gap (E_{el}) is found by adding the exciton binding energy (E_b) to the optical band gap (E_{opt}): $E_{el} = E_{opt} + E_b$

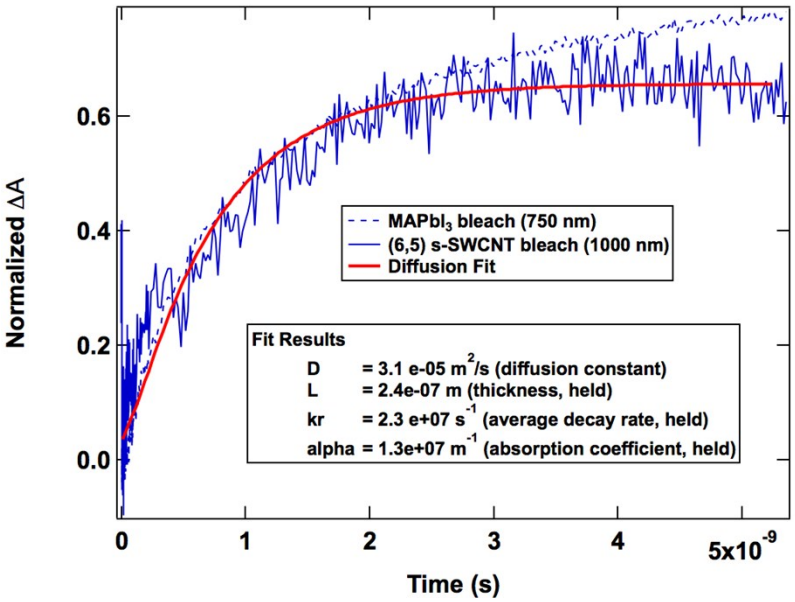

Figure S7. Modeling of the TA dynamics at 1000 nm (rise time of (6,5) s-SWCNT holes) and at 750 nm (loss of $MAPbI_3$ holes) for photoexcited trilayer sample (TiO_2/$MAPbI_3$/(6,5)-SWCNT) following photoexcitation at 400 nm.

$$N(t)=\frac{\alpha 2 n_0 L}{\pi}\exp(-kt)\sum_{m=0}^{\infty}\left(\exp\left(\frac{\pi^2 D}{L^2}\left(m+\frac{1}{2}\right)^2 t\right)\frac{\exp(-\alpha L)\pi\left(m+\frac{1}{2}\right)+(-1)^m \alpha L}{\left((\alpha L)^2+\pi^2\left(m+\frac{1}{2}\right)^2\right)\left(m+\frac{1}{2}\right)}\right)$$

Equation S1

Diffusion Modeling

The rise time of the (6,5) s-SWCNT bleach at 1000 nm was modeled to extract a hole diffusion length. First, the bleach was corrected for the fact that it is superimposed on the broad induced absorbance (IA) of the perovskite over the range of 900 – 1400 nm. To correct for this, the IA of the perovskite was subtracted away from the spectrum. To compare directly to the bleach recovery of the perovskite band-edge bleach, the corrected (6,5) bleach was then inverted so that the two traces would evolve with the same sign over the 5 ns window. The corrected/inverted (6,5) bleach was then scaled to match the normalized scaling of the perovskite bleach recovery.

The model used to fit the data is taken from Xing et al.,[3] who derived the analytical solution (Equation S1) to the one-dimensional diffusion equation for excitation conditions that are identical to the ones employed in our experiments – backside illumination with a quenching interface that is assumed to be a 100% efficient quencher. In Equation S1, α is the linear absorption coefficient of the active layer at the excitation wavelength (m^{-1}), L is the layer thickness (m), D is the charge carrier diffusion constant (m^2/s), k is the charge carrier decay constant (s^{-1}) associated with the intrinsic decay of carriers within the perovskite layer, and m is a summation integer. In our fit of the data, all variables were held except for the diffusion constant, D. The absorption coefficient at 400 nm was taken from Xing et al., $\alpha = 1.3 \times 10^7$ m^{-1}. The average decay constant, $k = 2.3 \times 10^7$ s^{-1}, was determined from the fit of the perovskite band-edge bleach, which yielded an average decay time of $\tau = 42$ ns. The active layer thickness, L, was held at 240 nm, as determined by profilometry.

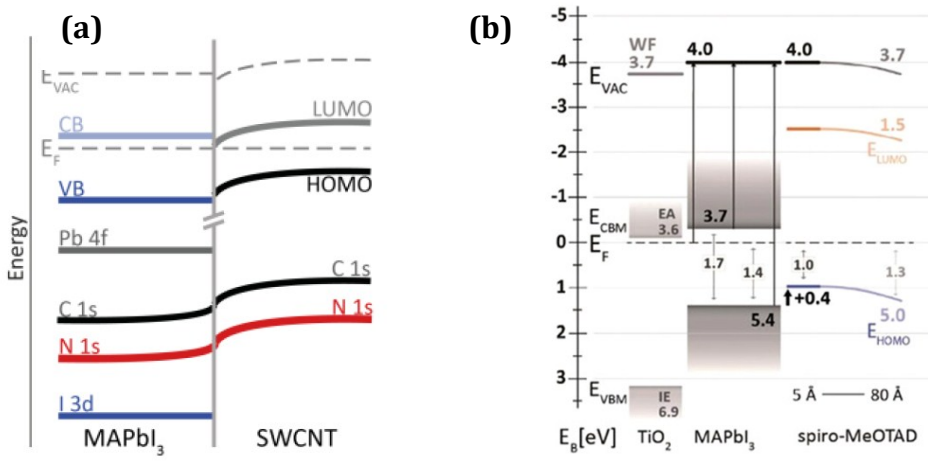

Figure S8. Summary of the interfacial band alignment obtained by photoelectron spectroscopy measurements for (a) MAPI/(6,5)-SWCNT interface (taken from Schulz et al.)[1], and (b) MAPI/spiro interface (taken from Schulz et al.)[2]. Note the opposite direction of band bending for each HTL, and that the band bending within the SWCNT HTL should provide an energetic barrier for back-transfer of holes to the MAPI valence band.

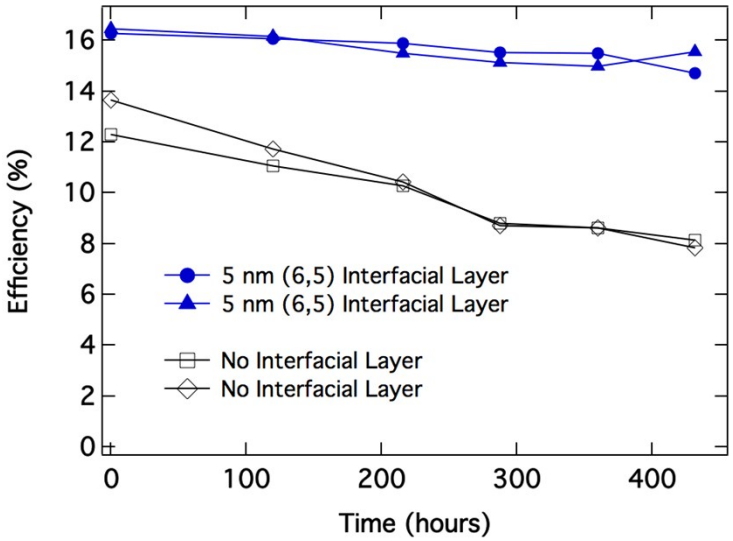

Figure S9. Representative stability experiments for devices prepared with or without 5 nm (6,5) s-SWCNT interfacial layers. Initial efficiencies for (6,5)-modified devices were 16.3% and 16.5%, and initial efficiencies for devices without (6,5) interfacial layers were 12.3% and 13.7%.

Table S1. Device parameters for $MAPbI_3$ solar cells prepared on an identical TiO_2 ETL and capped with a spiro-MeOTAD HTL. The devices either contained no interfacial layer or utilized (6,5) s-SWCNT interfacial layers with various thicknesses. All values are reported for forward scan.

Interfacial Layer	**$PCE_{forward}$ / $PCE_{reverse}$ (average)**
none	0.61
(6,5) 5 nm	0.76
(6,5) 10 nm	0.74
(6,5) 15 nm	0.64
None/toluene	0.55

Table S2. Ratio of power conversion efficiencies in forward and reverse direction for (6,5)-modified $MAPbI_3$ solar cells.

Interfacial Layer	**J_{sc} (avg) mA/cm^2**	**V_{oc} (avg) V**	**FF (avg)**	**PCE (avg) %**	**PCE (max) %**
none	20.1 ± 0.2	0.97 ± 0.03	0.44 ± 0.04	8.6 ± 0.7	9.6
(6,5) 5 nm	21.0 ± 0.3	1.05 ± 0.006	0.55 ± 0.02	12.2 ± 0.3	12.5
(6,5) 10 nm	20.1 ± 0.3	1.05 ± 0.002	0.52 ± 0.02	11.1 ± 0.2	11.7
(6,5) 15 nm	19.5 ± 0.5	1.01 ± 0.008	0.41 ± 0.03	8.0 ± 0.5	8.4
None/toluene	20.8 ± 0.01	1.01 ± 0.03	0.37 ± 0.03	7.9 ± 0.9	8.5

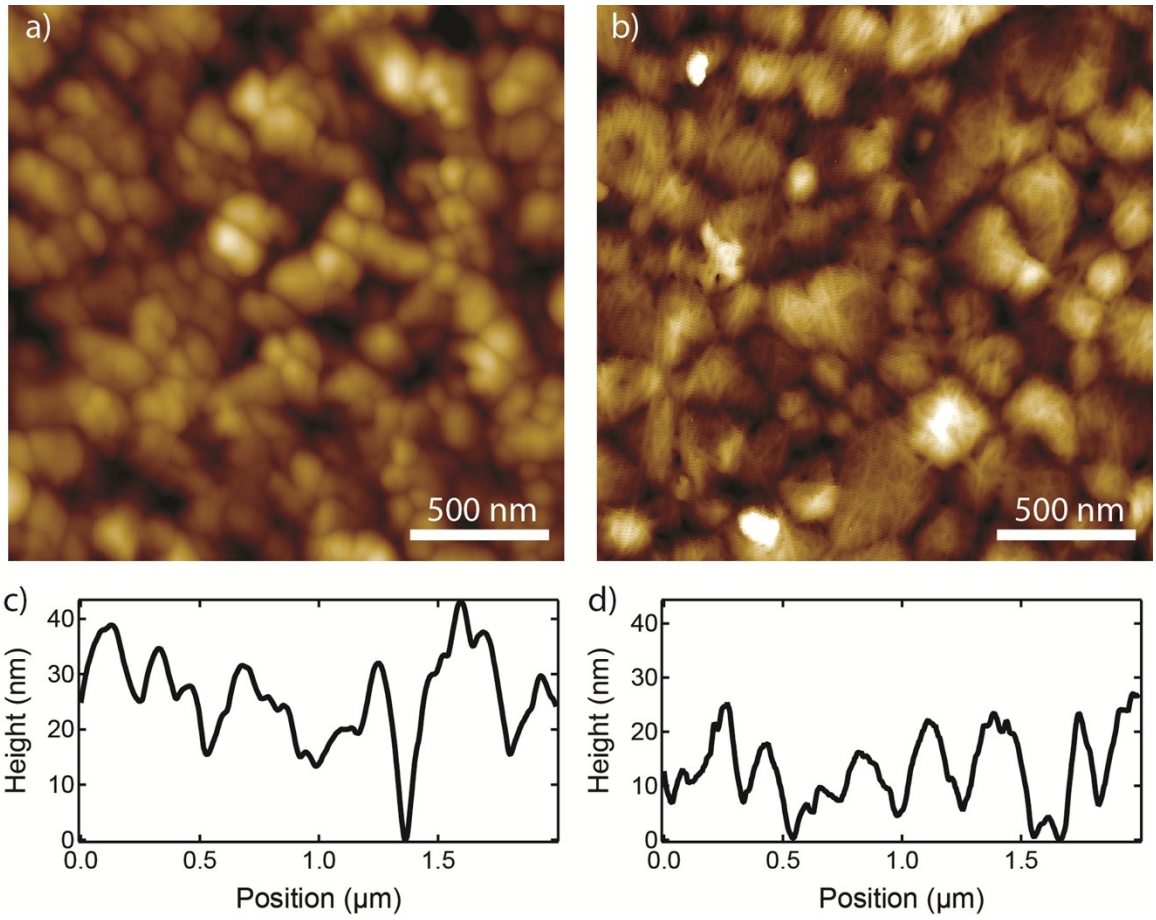

Figure S10. **(a) and (b)**: Atomic force microscopy topography images of **(a)** bare $MAPbI_3$ deposited onto FTO/TiO_2 and **(b)** 5 nm of LV SWCNTs deposited directly onto a $MAPbI_3$/TiO_2/FTO stack. **(c) and (d)**: Representative height profiles for **(c)** bare $MAPbI_3$ in image (a) and **(d)** SWCNT/$MAPbI_3$ surface in image (b).

Table S3. rms roughness measurements of $MAPbI_3$/SWCNT surfaces.

Sample[a]	rms surface roughness (nm)[b]
bare $MAPbI_3$	10
5 nm LV SWCNTs on $MAPbI_3$	11
10 nm LV SWCNTs on $MAPbI_3$	14
15 nm LV SWCNTs on $MAPbI_3$	18

[a] All samples were deposited onto a FTO/TiO_2 substrate.

[b] rms surface roughness values were obtained from a 15x15 μm^2 area for each sample.

References

1 Schulz, P.; Blackburn, J. L.; Berry, J. Charge Transfer Dynamics between Carbon Nanotubes and Hybrid Organic Metal Halide Perovskite Films *J. Phys. Chem. Lett.* **2015**, *Submitted,*

2 Schulz, P.; Edri, E.; Kirmayer, S.; Hodes, G.; Cahen, D.; Kahn, A. Interface Energetics in Organo-Metal Halide Perovskite-Based Photovoltaic Cells. *Energy & Environmental Science* **2014**, *7,* 1377-1381.

3 Xing, G.; Mathews, N.; Sun, S.; Lim, S. S.; Lam, Y. M.; Gratzel, M.; Mhaisalkar, S.; Sum, T. C. Long-Range Balanced Electron- and Hole-Transport Lengths in Organic-Inorganic Ch3nh3pbi3. *Science* **2013**, *342,* 344-347.